Physics Letters B 704 (2011) 343–346

Contents lists available at SciVerse ScienceDirect

Physics Letters B

www.elsevier.com/locate/physletb

Evolution of proto-neutron stars with the hadron–quark phase transition

Guo-yun Shao

INFN – Laboratori Nazionali del Sud, Via S. Sofia 62, I-95123 Catania, Italy

ARTICLE INFO

Article history:
Received 11 July 2011
Received in revised form 11 August 2011
Accepted 9 September 2011
Available online 16 September 2011
Editor: W. Haxton

Keywords:
Proto-neutron star
Trapped neutrino
Hadron–quark phase transition
Equation of state
Mass–radius relation

ABSTRACT

The Poyakov–Nambu–Jona-Lasinio (PNJL) model was developed recently, which includes both the chiral dynamics and (de)confinement effect and gives a good description of lattice QCD data. In this study we use the PNJL model to describe the quark phase, and first use it to study the evolution of proto-neutron star (PNS) with a hadron–quark phase transition. Along the line of a PNS evolution, we take several snapshots of PNS profiles, presenting the fractions of different species, the equations of state (EOS), and the mass–radius relations at different stages. The calculation shows the mixed phase may exist during the whole evolving process, and the onset density of quark phase decreases with the radiation of neutrinos in the heating stage. In the cooling stage, the EOS of the mixed phase softens and the center density increases. In this process a part of nuclear matter transforms to quark matter, which may lead to a PNS collapsing into a black hole.

Since the matter in the core of compact stars are compressed to densities of several times of saturated nuclear density, it is expected that new degrees of freedom will appear in the interior of these objects [1–13]. The hadron–quark phase transition is one of the most concerned topics in modern physics related to heavy-ion collision experiment and compact star. Because of the complication of full calculation of Quantum Chromodynamics (QCD) and the lack of sufficient knowledge about the nonpertubtive and (de)confinement effect, it is difficult to apply full QCD calculation to describe the phase transition in astrophysics. Therefore, in literatures the hadron–quark phase transition related to compact star are usually described with the simplified, phenomenological MIT bag model or the effective chiral Nambu–Jona-Lasinio (NJL) model (e.g., [7–9,11,14,16–19]).

The NJL model with chiral dynamics is a prominent one in the application of astrophysics, but it lacks the confinement mechanism, one essential characteristic of QCD. Recently, an improved version of the NJL model coupled to Polyakov loop (PNJL) has been proposed [20]. The PNJL model includes both the chiral dynamic and (de)confinement effect, giving a good interpretation of lattice QCD data [21–27]. We have recently studied the hadron–quark phase transition relevant to heavy-ion collision in the Hadron-PNJL model [28]. The calculation shows the color (de)confinement effect is very important for the hadron–quark phase transition at finite density and temperature, and improves greatly the results derived from the Hadron-NJL model [29]. The PNJL model with a chemical potential dependent Poyakov effective potential has also been used to describe cold neutron star without [30] and with a color superconductivity structure [31]. In [32], Fischer et al. discussed the evolution of core collapse supernova with the PNJL model (with diquark interaction and isoscalar vector interaction) and the possibility of the onset of deconfinement in core collapse supernova simulation. In their study selected proton-to-baryon ratio Y_p and the Maxwell construction are taken for the PNJL model, which gives a relatively narrow mixed phase than that with Gibbs construction. In [33], the authors studied the possibility to probe the QCD critical endpoint during the dynamical black hole formation from a gravitational collapse. Several two-flavor quark models with different parameters are used in their study, and the calculation shows the Critical Point location of QCD has a strong dependence on quark models and parameters. A generalization with s quark is needed to get more reliable results for further investigation.

In this Letter we will firstly use the newly improved PNJL model to describe the evolution of proto-neutron star from its birth with trapped neutrinos to neutrino-free cold neutron star (NS). The Gibbs criteria will be used to determine the mixed phase under the isotropic constraint with and without trapped neutrinos. The emphases are put on the evolution of proto-neutron star with a hadron–quark phase transition, the particle distributions along baryon density, the EOSs and mass–radius relations, as well as the star stability in different snapshots during the evolution.

A PNS forms after the gravitational collapse of the core of massive star with the explosion of a supernova. At the beginning of the birth of a PNS, the entropy per baryon is about one ($S \simeq 1$) and the number of leptons per baryon with trapped neutrino is

E-mail address: shaogy@pku.edu.cn.

0370-2693
doi:10.1016/j.physletb.2011.09.030

approximate 0.4 ($Y_{Le} = Y_e + Y_{\nu_e} \simeq 0.4$). In the following 10–20 seconds, neutrinos escape from the star. With the decrease of electron neutrino population, the star matter is heated by the diffusing neutrinos, and the corresponding entropy density increases, reaching to $S \simeq 2$ when $Y_{\nu e} \simeq 0$. Following the heating, the star begins cooling by radiating neutrino pairs of all flavors, and finally a cold neutrons forms [34,35].

Along the line of a PNS evolution to the formation of a cold neutron star, we take several snapshots to study how the star evolves, especially with the appearance of quark degrees of freedom. The snapshots are taken with the following conditions ($S = 1, Y_{Le} = Y_e + Y_{\nu_e} = 0.4$), ($S = 1.5, Y_{Le} = Y_e + Y_{\nu_e} = 0.3$), ($S = 2, Y_{\nu_e} = 0$) and ($S = 0, Y_{\nu_e} = 0$), similar with that used in [34,35]. At each snapshot of a PNS evolution, we take an isentropic approximation with which the temperature has a radial gradient in the star. There are also studies related to the properties of PNS based on isothermal approximation (e.g., [15,17–19]).

For the star matter, the hadronic and quark phase are described by the non-linear Walecka model and the PNJL model, respectively. In the mixed phase between pure hadronic and quark matter, the two phases are connected to each other by the Gibbs conditions deduced from thermal, chemical and mechanical equilibriums. For the hadron phase we use the Lagrangian given in [36] in which the interactions between nucleons are mediated by σ, ω, ρ mesons, and the parameter set GM1 is used in the calculation. The details can be found in Refs. [36,5].

For the quark phase, we take recently developed three-flavor PNJL model with the Lagrangian density

$$\begin{aligned}\mathcal{L}_q = {}& \bar{q}\big(i\gamma^\mu D_\mu - \hat{m}_0\big)q + G\sum_{k=0}^{8}\big[(\bar{q}\lambda_k q)^2 + (\bar{q}i\gamma_5\lambda_k q)^2\big] \\ & - K\big[\det{}_f\big(\bar{q}(1+\gamma_5)q\big) + \det{}_f\big(\bar{q}(1-\gamma_5)q\big)\big] \\ & - \mathcal{U}\big(\Phi[A], \bar{\Phi}[A], T\big), \end{aligned} \tag{1}$$

where q denotes the quark fields with three flavors, u, d, and s, and three colors; $\hat{m}_0 = \mathrm{diag}(m_u, m_d, m_s)$ in flavor space; G and K are the four-point and six-point interacting constants, respectively. The four-point interaction term in the Lagrangian keeps the $SU_V(3) \times SU_A(3) \times U_V(1) \times U_A(1)$ symmetry, while the 't Hooft six-point interaction term breaks the $U_A(1)$ symmetry.

The covariant derivative in the Lagrangian is defined as $D_\mu = \partial_\mu - iA_\mu$. The gluon background field $A_\mu = \delta^0_\mu A_0$ is supposed to be homogeneous and static, with $A_0 = g\mathcal{A}^\alpha_0 \frac{\lambda^\alpha}{2}$, where $\frac{\lambda^\alpha}{2}$ is $SU(3)$ color generators. The effective potential $\mathcal{U}(\Phi[A], \bar{\Phi}[A], T)$ is expressed in terms of the traced Polyakov loop $\Phi = (\mathrm{Tr}_c\, L)/N_C$ and its conjugate $\bar{\Phi} = (\mathrm{Tr}_c\, L^\dagger)/N_C$. The Polyakov loop L is a matrix in color space

$$L(\vec{x}) = \mathcal{P}\exp\left[i\int_0^\beta d\tau\, A_4(\vec{x}, \tau)\right], \tag{2}$$

where $\beta = 1/T$ is the inverse of temperature and $A_4 = iA_0$.

Different effective potentials were adopted in literatures [21,37,38,30]. The modified chemical dependent one

$$\begin{aligned}\mathcal{U} = {}& \big(a_0T^4 + a_1\mu^4 + a_2T^2\mu^2\big)\Phi^2 \\ & \times a_3T_0^4\ln\big(1 - 6\Phi^2 + 8\Phi^3 - 3\Phi^4\big)\end{aligned} \tag{3}$$

was used in [30,31] which is a simplification of

$$\begin{aligned}\mathcal{U} = {}& \big(a_0T^4 + a_1\mu^4 + a_2T^2\mu^2\big)\bar{\Phi}\Phi \\ & \times a_3T_0^4\ln\big[1 - 6\bar{\Phi}\Phi + 4\big(\bar{\Phi}^3 + \Phi^3\big) - 3(\bar{\Phi}\Phi)^2\big]\end{aligned} \tag{4}$$

because the difference between $\bar{\Phi}$ and Φ is smaller at finite chemical potential and $\bar{\Phi} = \Phi$ at $\mu = 0$. In the calculation we will use the later one. The related parameters, $a_0 = -1.85$, $a_1 = -1.44 \times 10^{-3}$, $a_2 = -0.08$, $a_3 = -0.4$, are still taken from [30], which can reproduce well the data obtained in lattice QCD calculation.

In the mean field approximation, quarks can be taken as free quasiparticles with constituent masses M_i, and the dynamical quark masses (gap equations) are obtained as

$$M_i = m_i - 4G\phi_i + 2K\phi_j\phi_k \quad (i \neq j \neq k), \tag{5}$$

where ϕ_i stands for quark condensate. The thermodynamic potential of the PNJL model in the mean field level can be derived as

$$\begin{aligned}\Omega = {}& \mathcal{U}(\bar{\Phi}, \Phi, T) + 2G\big({\phi_u}^2 + {\phi_d}^2 + {\phi_s}^2\big) \\ & - 4K\phi_u\,\phi_d\,\phi_s - 2\int_\Lambda \frac{\mathrm{d}^3p}{(2\pi)^3}3(E_u + E_d + E_s) \\ & - 2T\sum_{u,d,s}\int \frac{\mathrm{d}^3p}{(2\pi)^3}\ln\big[A(\bar{\Phi}, \Phi, E_i - \mu_i, T)\big] \\ & - 2T\sum_{u,d,s}\int \frac{\mathrm{d}^3p}{(2\pi)^3}\ln\big[\bar{A}(\bar{\Phi}, \Phi, E_i + \mu_i, T)\big],\end{aligned} \tag{6}$$

where

$$\begin{aligned}A(\bar{\Phi}, \Phi, E_i - \mu_i, T) = {}& 1 + 3\Phi e^{-(E_i-\mu_i)/T} + 3\bar{\Phi}e^{-2(E_i-\mu_i)/T} \\ & + e^{-3(E_i-\mu_i)/T}\end{aligned}$$

and

$$\begin{aligned}\bar{A}(\bar{\Phi}, \Phi, E_i + \mu_i, T) = {}& 1 + 3\bar{\Phi}e^{-(E_i+\mu_i)/T} + 3\Phi e^{-2(E_i+\mu_i)/T} \\ & + e^{-3(E_i+\mu_i)/T}.\end{aligned}$$

The values of ϕ_u, ϕ_d, ϕ_s, Φ and $\bar{\Phi}$ are determined by minimizing the thermodynamical potential

$$\frac{\partial\Omega}{\partial\phi_u} = \frac{\partial\Omega}{\partial\phi_d} = \frac{\partial\Omega}{\partial\phi_s} = \frac{\partial\Omega}{\partial\Phi} = \frac{\partial\Omega}{\partial\bar{\Phi}} = 0. \tag{7}$$

All the thermodynamic quantities relevant to the bulk properties of quark matter can be obtained from Ω. Particularly, the pressure and entropy density can be derived with $P = -(\Omega(T,\mu) - \Omega(0,0))$ and $S = -\partial\Omega/\partial T$, respectively.

As an effective model, the (P)NJL model is not renormalizable, so a cut-off Λ is implemented in 3-momentum space for divergent integrations. The model parameters: $\Lambda = 603.2$ MeV, $G\Lambda^2 = 1.835$, $K\Lambda^5 = 12.36$, $m_{u,d} = 5.5$ and $m_s = 140.7$ MeV, determined by fitting f_π, M_π, m_K and m_η to their experimental values [39], are used in the calculation.

The Gibbs criteria is usually implemented for a complicated system with more than one conservation charge. The Gibbs conditions for the mixed phase of hadron–quark phase transition in compact star are

$$\mu^H_\alpha = \mu^Q_\alpha, \qquad T^H = T^Q, \qquad P^H = P^Q, \tag{8}$$

where μ_α are usually chosen with μ_n and μ_e. Under the β equilibrium with trapped neutrino, the chemical potential of other particles including all baryons, quarks, and leptons can be derived by

$$\mu_i = b_i\mu_n - q_i\mu_e + q_i\mu_{\nu_e}, \tag{9}$$

where b_i and q_i are the baryon number and electric charge number of particle species i, respectively. For the matter with trapped electron neutrinos, $Y_{L\mu} = (Y_\mu + Y_{\nu_\mu}) \simeq 0$, we do not need to consider the contribution from muon and muon neutrino [34,35]. For

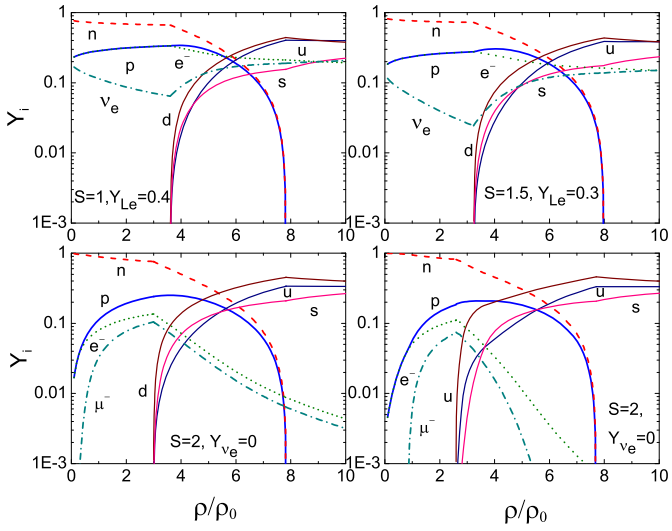

Fig. 1. Relative fractions of different species as functions of baryon density at several snapshots of a PNS evolution. The upper (lower) panels are the results with (without) trapped neutrinos.

the neutrino-free matter ($\mu_{\nu_e} = 0$), both electrons and muons are included in the calculation.

The baryon number density and energy density in the mixed phase are composed of two parts with the following combinations

$$\rho = (1-\chi)\rho_B^H + \chi\rho_B^Q, \tag{10}$$

and

$$\varepsilon = (1-\chi)\varepsilon^H + \chi\varepsilon^Q, \tag{11}$$

where χ is the volume fraction of quark matter. And the electric neutrality is fulfilled globally with

$$q_{total} = (1-\chi)\sum_{i=B,l} q^i\rho_i + \chi\sum_{i=q,l} q^i\rho_i = 0. \tag{12}$$

In Fig. 1, we display the relative fractions of different species as functions of baryon density in several snapshots along the evolution of a proto-neutron star, from ($S = 1, Y_{Le} = Y_e + Y_{\nu_e} = 0.4$), ($S = 1.5, Y_{Le} = Y_e + Y_{\nu_e} = 0.3$), ($S = 2$, $Y_{\nu_e} = 0$) to cold neutron star with ($S = 0, Y_{\nu_e} = 0$). Comparing the upper panels with trapped neutrino with the lower panels without trapped neutrino, we find that the fraction of trapped neutrino affects the proton–neutron ratio Y_p/Y_n at lower density before the appearance of quarks. For the hot PNS matter, Y_p/Y_n with rich ν_e is larger than that with poor ν_e. According to the Pauli principle, the smaller Y_p/Y_n will excite more neutrons to occupy higher energy levels, leading to a stiffer equation of state.

Another point we stress is that the onset density of quark phase decreases with the escape of trapped neutrinos, i.e., trapped neutrinos delay the hadron–quark phase transition to a higher density. For the neutrino-trapped matter, the fraction of neutrino is enhanced with the appearance of quarks, which also affects the neutrino opacity. For neutrino-free cases, the lepton population in cold neutron star matter ($S = 0, Y_{\nu_e} = 0$) is smaller than that of PNS ($S = 2, Y_{\nu_e} = 0$), especially after the appearance of quarks at high density.

The largest center densities of proto-neutron stars at the first three snapshots taken above are $\rho_c = 5.23, 5.00$, and $4.54\rho_0$, respectively. The center density decreases with the radiation of neutrinos, because the star expands when the inner matter is heated by the escaped neutrinos. When neutrinos are free, the PNS begins cooling by radiating neutrino pairs of all flavor and the star shrinks

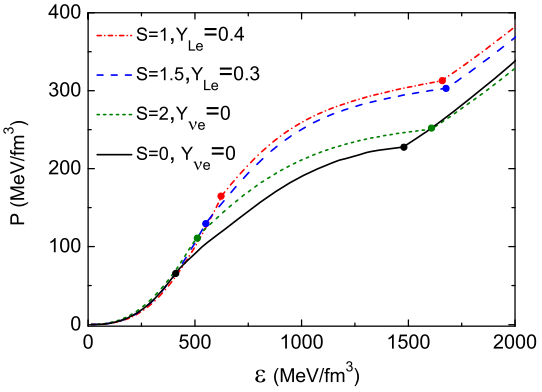

Fig. 2. EOSs of PNS and NS matter at several stages of the star evolution. The dots mark the range of the mixed phase.

until the formation of cold neutron star. During the cooling stage, the center density of the star increases. The center density of cold neutron star is $\rho_c = 4.88\rho_0$. The variation of the center densities during a PNS evolution is easier to understand by combining the mass–radius relations that will be given latterly.

We present the equations of state of the star matter at different evolving stages in Fig. 2. The dots mark the ranges of the mixed phases. For the PNS matter at low density before the onset of quarks, the EOS becomes more and more stiffer with the decrease of lepton fraction and the increase of entropy density. This mainly attributes to the decreased Y_p/Y_n, as shown in Fig. 1, which excites more neutrons to higher energy states. In contrast, the EOS of the mixed phase with a larger lepton fraction is much stiffer. This is because the pure quark phase has a stiffer EOS, but the corresponding hadron phase with the same lepton fraction and entropy density has a softer one. To fulfill the Gibbs condition of the chemical and mechanical equilibrium, the phase transition can only take place at relatively larger energy density. For the case with a stiffer hadronic EOS at lower density, the Gibbs condition can be realized at lower energy density to drive the hadron–quark phase transition. The similar results have been obtained when the NJL model is taken [34]. The cold neutron star matter at lower density has an EOS between the initial conditions and the end of heating stage, and a softest one for the mixed phase after quarks appearing.

Comparing the results obtained in the NJL model in [34], we find the pressure of the mixed phase of a PNS given by the PNJL model is larger than that of NJL model. This reflects that the confinement effect (gluon field) is important at finite temperature. With the PNJL model, the pressure of quark matter at finite temperature are much smaller than that of NJL model, therefore the phase transition can only take place at relatively larger density to assure the quark-phase pressure can match that of the hadron phase. The details can be found in Refs. [28,29] where the hadron–quark phase transition for symmetric and asymmetric matter related to heavy-ion collision experiment has been investigated in the Hadron-(P)NJL model, and the same results were obtained.

The above illustration also explains the inverse of pressure of the mixed phase in the cases of ($S = 2, Y_{\nu_e} = 0$) and ($S = 0, Y_{\nu_e} = 0$) as given by the NJL model in [34]. All the features of equations of state will be reflected in the mass–radius relations.

Finally, in Fig. 3 we plot the mass–radius relations of several snapshots taken above along the evolution a PNS. This figure gives us a more intuitive picture about the PNS evolution with a hadron–quark phase transition. Firstly, in the heating stage the PNS expands with the decrease of lepton fraction (Y_{Le}) and the increase of entropy density (S). Simultaneously, the center density decreases with the expansion of the star. When neutrinos are free, the star begins cooling, and then the star shrinks, leading to the

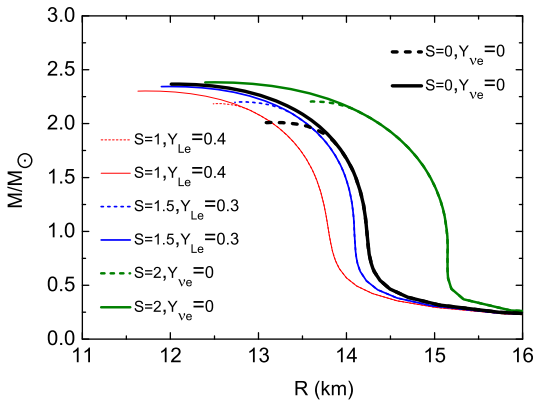

Fig. 3. Mass–radius relations of PNS and NS at several snapshots along a PNS evolution. The solid curves are the results without quarks and the dash curves are the results with hadron–quark phase transition.

center density increasing again. In this stage for a star with quarks, a part of nuclear matter transforms to quark matter and the EOS becomes softer in the mixed phase. The star may collapse into a black hole in the cooling process if the EOS in the core cannot resist the gravity. This point is different from the result derived in the NJL model.

The radio timing observations of the binary millisecond pulsar J1614-2230 with a strong general relativistic Shapiro delay signature, implies that the pulsar mass is $1.97 \pm 0.04 M_{\odot}$ [40]. The discovery of this massive pulsar rules out many soft equations of state. With the improved quark model, our calculation shows the maximum mass of cold neutron star with deconfined quarks is slightly larger than $2M_{\odot}$. Because the quark model parameters are determined by experiments and lattice QCD simulation, a stiffer hadronic EOS is needed to fulfill this constraint. On the other hand, If a vector interaction is included for quark matter, the EOS will be stiffer and the maximum mass of hybrid star will be improved.

In summary, we have studied the evolution of PNS with a hadron–quark phase transition with a more reliable quark model including both chiral dynamics and (de)confinement effect. The calculation shows the quark phase may exist in the whole process of a PNS evolution. The trapped neutrinos affect greatly the ration of Y_p/Y_n and the EOS at low density before quarks appearing. In the heating stage, with the deleptonization and the increase of entropy density, the PNS expands and the corresponding center density decreases. In contrast, in the cooling stage, the PNS shrinks and the center density increases. During this process a part of nuclear matter transforms to quark matter, and the PNS may collapse into a black hole if the EOS in the core is not stiff enough.

In this study, only the $\bar{q}q$ interaction is considered for quark phase because the relevant model parameters can be fixed with experiments and lattice QCD simulation. In analogy to BCS theory, color superconductivity in low-temperature and high-density QCD matter may appear and there may exist rich phase diagram. The coupling constant of this interaction channel affects the equation of state of quark matter and the onset density of quark phase in compact star. One question is that the coupling parameter cannot be fixed from heavy-ion experiment or lattice QCD simulation. On the other hand, the (isoscalar) vector interaction channel has been included in some studies. Such an interaction reduces the effective quark chemical potential but contributes to the pressure of quark matter. This interaction stiffens the EOS of quark matter and increases the maximum mass of a hybrid star. Compared with the hadron Walecka model, the (isoscalar) vector interaction in quark matter plays the role corresponding to the ω meson. One drawback is that the coupling constant is usual taken as a free parameter and its strength affects greatly the Critical End Point of chiral symmetry restoration relevant to heavy-ion collision experiment. Besides, the isovector vector interaction (corresponding to the role of ρ meson in hadron phase and influencing the symmetry energy of quark matter) can be also introduced for asymmetric quark matter. For these interaction channels as well as hyperon degrees of freedom, the difficulty is the uncertainties of the relevant coupling parameters with the lack of experiment data, so we temporarily omit these interactions in this study. And a systematic investigation on these problems is in progress as a further study.

References

[1] N.K. Glendenning, J. Schaffner-Bielich, Phys. Rev. Lett. 81 (1998) 4564;
N.K. Glendenning, J. Schaffner-Bielich, Phys. Rev. C 60 (1999) 025803;
J. Schaffner, I.N. Mishustin, Phys. Rev. C 53 (1996) 1416;
J. Schaffner-Bielich, Nucl. Phys. A 804 (2008) 309.
[2] D.P. Menezes, P.K. Panda, C. Providência, Phys. Rev. C 72 (2005) 035802.
[3] G.E. Brown, C.H. Lee, H.J. Park, M. Rho, Phys. Rev. Lett. 96 (2006) 062303.
[4] T. Maruyama, T. Tatsumi, D.N. Voskresensky, T. Tanigawa, T. Endo, S. Chiba, Phys. Rev. C 73 (2006) 035802.
[5] G.Y. Shao, Y.X. Liu, Phys. Rev. C 79 (2009) 025804;
G.Y. Shao, Y.X. Liu, Phys. Rev. C 82 (2010) 055801;
G.Y. Shao, Y.X. Liu, Phys. Lett. B 682 (2009) 171.
[6] T. Muto, Nucl. Phys. A 754 (2005) 350;
T. Muto, Phys. Rev. C 77 (2008) 015810.
[7] D.B. Blaschke, H. Grigorian, G. Poghosyan, C.D. Roberts, S. Schmidt, Phys. Lett. B 450 (1999) 207;
D. Blaschke, et al., Phys. Rev. D 72 (2005) 065020.
[8] M. Baldo, et al., Phys. Lett. B 562 (2003) 153.
[9] F. Weber, Prog. Part. Nucl. Phys. 54 (2005) 193.
[10] M. Alford, M. Braby, M. Paris, S. Reddy, Astrophys. J. 629 (2005) 969;
M. Alford, D.B. Blaschke, A. Drago, T. Klähn, G. Pagliara, J. Shaffner-Bielich, Nature 445 (2007) E7.
[11] F. Yang, H. Shen, Phys. Rev. C 77 (2008) 025801.
[12] J.M. Lattimer, M. Prakash, Phys. Rep. 442 (2007) 109.
[13] T. Klähn, D. Blaschke, F. Sandin, et al., Phys. Lett. B 654 (2007) 170.
[14] G. Pagliara, M. Hempel, J. Schaffner-Bielich, Phys. Rev. Lett. 103 (2009) 171102;
K. Schertler, S. Leupold, J. Schaffner-Bielich, Phys. Rev. C 60 (1999) 025801.
[15] G.F. Burgio, S. Plumari, Phys. Rev. D 77 (2008) 085022;
O.E. Nicotra, M. Baldo, G.F. Burgio, H.J. Schulze, Phys. Rev. D 74 (2006) 123001.
[16] M. Buballa, F. Neumann, M. Oertel, I. Shovkovy, Phys. Lett. B 595 (2004) 36.
[17] N. Yasutake, K. Kashiwa, Phys. Rev. D 79 (2009) 043012.
[18] M.G. Paoli, D.P. Menezes, Eur. Phys. J. A 46 (2010) 413;
D.P. Menezes, C. Providência, Phys. Rev. C 68 (2003) 035804.
[19] I. Bombaci, D. Logoteta, C. Providência, I. Vidaña, Astron. Astrophys. 528 (2011) A71.
[20] K. Fukushima, Nucl. Phys. B 591 (2004) 277.
[21] C. Ratti, M.A. Thaler, W. Weise, Phys. Rev. D 73 (2006) 014019.
[22] P. Costa, M.C. Ruivo, C.A. de Sousa, H. Hansen, Symmetry 2 (3) (2010) 1338.
[23] B.-J. Schaefer, M. Wagner, J. Wambach, Phys. Rev. D 81 (2010) 074013.
[24] T.K. Herbst, J.M. Pawlowski, B.-J. Schaefer, Phys. Lett. B 696 (2011) 58.
[25] K. Kashiwa, H. Kouno, M. Matsuzaki, M. Yahiro, Nucl. Phys. B 662 (2008) 26.
[26] H. Abuki, R. Anglani, R. Gatto, G. Nardulli, M. Ruggieri, Phys. Rev. D 78 (2008) 034034.
[27] W.J. Fu, Z. Zhang, Y.X. Liu, Phys. Rev. D 77 (2008) 014006.
[28] G.Y. Shao, M. Di Toro, V. Greco, M. Colonna, S. Plumari, B. Liu, Y.X. Liu, Phys. Rev. D 84 (2011) 034028.
[29] G.Y. Shao, M. Di Toro, B. Liu, M. Colonna, V. Greco, Y.X. Liu, S. Plumari, Phys. Rev. D 83 (2011) 094033.
[30] V.A. Dexheimer, S. Schramm, Phys. Rev. C 81 (2010) 045201;
V.A. Dexheimer, S. Schramm, Nucl. Phys. B 199 (2010) 319;
R. Negreiros, V.A. Dexheimer, S. Schramm, Phys. Rev. C 82 (2010) 035803.
[31] D. Blaschke, J. Berdermann, R. Łastowiecki, Prog. Theor. Phys. Suppl. 186 (2010) 81.
[32] T. Fischer, et al., arXiv:1103.3004v2.
[33] A. Ohnishi, et al., arXiv:1102.3753v1.
[34] A.W. Steiner, M. Praskash, J.M. Lattimer, Phys. Lett. B 486 (2000) 239.
[35] S. Reddy, M. Praskash, J.M. Lattimer, Phys. Rev. D 58 (1998) 013009.
[36] N.K. Glendenning, S.A. Moszkowski, Phys. Rev. Lett. 67 (1991) 2414;
N.K. Glendenning, Compact Stars, Springer-Verlag, Berlin, 2000.
[37] S. Rößner, C. Ratti, W. Weise, Phys. Rev. D 75 (2007) 034007.
[38] K. Fukushima, Phys. Rev. D 77 (2008) 114028.
[39] P. Rehberg, S.P. Klevansky, J. Hüfner, Phys. Rev. C 53 (1995) 410.
[40] P.B. Demorest, T. Pennucci, S.M. Ransom, M.S.E. Roberts, J.W.T. Hessels, Nature 467 (2010) 1081.